Proceedings of the 11th World Congress on Civil, Structural, and Environmental Engineering (CSEE 2026)
Paris, France - April, 2026
Paper No. ICSECT 151
DOI: 10.11159/icsect26.151

Enhancing Self-Heating Efficiency of Concrete Through Continuous Carbon Fiber Architectures

Rawan ALSAMORI[1] and Murat OZTURK[1]*
[1] Smart Materials Laboratory, Bursa Uludag University, Engineering Faculty, Department of Civil Engineering, Bursa, Türkiye
***Corresponding author - email:** muratozturk@uludag.edu.tr

Abstract **-** Cementitious composites generally lack electrical conductivity, which limits their use in multifunctional applications such as self-heating systems. This study investigates the self-heating performance of concrete reinforced with continuous carbon fiber bundles, with emphasis on the effects of fiber configuration and placement density. Four continuous carbon fiber bundles were embedded into concrete specimens in straight, twisted, and braided configurations, combined with low (L), medium (M), and high (H) placement densities. Self-heating behavior was evaluated under applied AC voltages of 30 V and 45 V by monitoring surface temperature evolution using infrared thermography and recording electrical power consumption. The results showed that both fiber configuration and placement density significantly influence electrical network continuity and Joule heating performance. In particular, braided–high and twisted–high configurations exhibited the most efficient and stable self-heating behavior at both voltage levels, whereas low and medium density arrangements resulted in limited temperature increase. The findings demonstrate that the use of densely arranged continuous carbon fiber bundles, especially in braided configurations, provides an effective approach for developing self-heating cementitious composites suitable for infrastructure and building applications.

Keywords**:** Self-heating concrete; Continuous carbon fibers; Fiber configuration; Joule heating; Multifunctional cementitious composites

1. Introduction

Cementitious composites are among the most widely used construction materials in the building industry. They are preferred due to their adequate mechanical strength, durability, cost-effectiveness, and ease of production [1]. However, with the increasing demands of modern life, the high load-bearing capacity provided by cementitious composites alone is no longer considered sufficient. Instead, contemporary engineering approaches require these materials to simultaneously exhibit additional functionalities. Materials capable of performing more than one function are commonly referred to as multifunctional materials [2–5]. Self-cleaning [6,7], self-healing [8,9], self-sensing [10,11], radiation shielding [12,13], and self-heating [14,15] are among the most prominent functionalities investigated in cement-based systems.

Cementitious composites are inherently electrically insulating due to their microstructural characteristics [16]. In order to enable functionalities such as self-sensing, electromagnetic radiation shielding, and self-heating, electrical conductivity must be introduced into the composite matrix. This is commonly achieved by incorporating highly conductive materials into the cementitious system. Carbon-based conductive fillers, including carbon black [17], graphene [18], carbon nanotubes [19], and carbon fibers [20], are widely reported in the literature as effective additives for enhancing the electrical properties of cement-based composites.

The self-heating capability of cementitious composites is based on the principle of resistive heating, where heat is generated as a result of electrical current passing through an electrically conductive network within the material. This phenomenon is commonly referred to as Joule heating [21]. Cementitious composites endowed with self-heating functionality are considered promising for various applications, including indoor heating systems in buildings, bridge decks, airport runways, and pavement structures designed to prevent ice formation under cold climate conditions.

Numerous studies reported in the literature demonstrate that self-heating functionality is commonly achieved by randomly dispersing discontinuous conductive fillers throughout the cementitious matrix [22–25]. However, such approaches often result in limited electrical network continuity and require relatively high filler contents to achieve sufficient conductivity. In the present study, an alternative approach is adopted. Carbon fibers are not randomly dispersed as short, discontinuous elements but are instead introduced into the concrete matrix as continuous fiber bundles arranged in strip form. These bundles are physically configured into different geometrical forms, including straight, twisted, and braided arrangements. The influence of these fiber configurations on the electrical and thermal performance of the composite is systematically investigated.

Within the scope of this study, the effects of fiber configuration and placement density on the electrical and thermal behavior of concrete specimens are examined in a systematic manner. An experimental program is designed in which continuous carbon fibers are arranged in three different configurations, namely straight (S), twisted (T), and braided (B), and combined with three placement densities, defined as low (L), medium (M), and high (H). The water-to-cement ratio is kept constant for all mixtures. Electrical potentials of 30 V and 45 V are applied to the specimens, and the temperature evolution and power consumption are monitored over time. Through these measurements, the effects of fiber configuration and placement density on electrical network formation and Joule heating performance within the concrete matrix are evaluated in detail

2. Materials and method

Continuous carbon fiber bundles are used as conductive elements in this study. Carbon fibers are provided by DowAksa (Yalova, Türkiye). Three different fiber configurations are considered: untreated (straight), twisted, and braided. The untreated fiber bundles are used as received and serve as the reference configuration. Twisted fiber bundles are produced by applying controlled torsional deformation along the longitudinal axis of the bundle. Three different twist densities, defined as low, medium, and high, are obtained by varying the number of twists per unit length. Braided fiber bundles are produced by interlacing multiple carbon fiber strands into a braided structure, and three different braiding densities are achieved by adjusting the braid tightness. These configurations are selected to systematically modify fiber–fiber contact, electrical pathway continuity, and current distribution within the conductive network, as schematically illustrated in Figure 1.

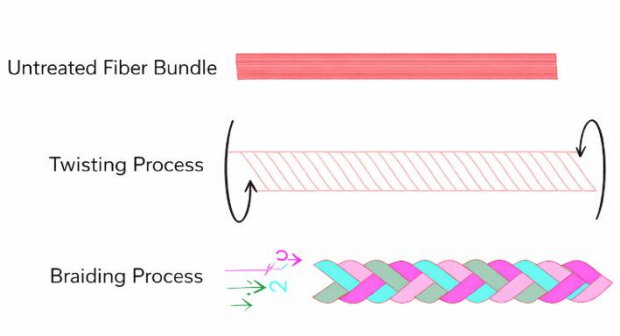

Figure 1. Schematic illustration of continuous carbon fiber bundle configurations: untreated (straight), twisted, and braided.

Concrete specimens are cast in prismatic molds with internal dimensions of 150 × 150 × 50 mm³. Carbon fiber bundles are cut to a length of 150 mm, matching the specimen length to ensure continuous conductive pathways along the loading direction. Each fiber bundle consists of 72,000 individual filaments (72k), with an average single-fiber diameter of approximately 7 μm. In all specimens, four carbon fiber bundles are embedded as continuous and parallel strips aligned along the longitudinal direction of the specimen. The bundles are positioned symmetrically within the cross-section. To minimize contact resistance and ensure stable electrical current transfer, conductive silver paint is applied to the exposed ends of the carbon fiber bundles. The silver paint is allowed to dry at room temperature, after which electrical clamps are attached to establish reliable and repeatable electrical connections. Pictures of the fiber placement are shown in Figure 2.



Figure 2. Configuration of continuous carbon fiber bundles embedded in concrete specimens to establish continuous conductive pathways.

Concrete mixtures are prepared using Ordinary Portland cement, aggregates, and potable water with a fixed cement : aggregate : water ratio of 1 : 3 : 0.5. No chemical admixtures are used. Concrete placement is carried out in two stages to ensure accurate and repeatable fiber positioning. Initially, approximately half of the fresh concrete is poured into the mold and allowed to reach the initial setting stage. After initial setting, the carbon fiber bundles are carefully placed onto the partially set concrete surface at predefined locations. Subsequently, the remaining concrete is poured into the mold to fully embed the fiber bundles. Mechanical vibration is applied after the final casting stage to ensure proper consolidation and to eliminate entrapped air while preventing fiber floating or displacement. After casting, specimens are demolded after 24 hours and cured under controlled laboratory conditions until testing.

Self-heating performance is evaluated by applying alternating current (AC) to the specimens through the embedded carbon fiber bundles using an AC power supply (GW Instek ASR-2050). AC voltage levels of 30 V and 45 V are applied during testing. Electrical current and power consumption are recorded continuously as functions of time. The thermal response of the specimens is characterized by tracking surface temperature development and heat distribution using an infrared imaging system. A Fluke TiS75+ thermal camera is employed and mounted normal to the specimen surface at a constant separation of 0.50 m. The device operates within a temperature interval of −20 °C to 550 °C and provides a spatial resolution of 384 × 288 pixels. Thermal data are recorded via FLUKE Connect software, and mean surface temperatures are determined by averaging over the entire exposed area of the specimen. An emissivity coefficient of 0.95, representative of cement-based materials, is adopted. Environmental conditions are kept approximately stable during testing. To ensure measurement consistency and repeatability, camera orientation, distance, and emissivity settings are maintained identical for all specimens. The overall measurement configuration is illustrated in Figure 3. Table 1 shows specimen geometry, fiber properties, and experimental variables for the test specimens.

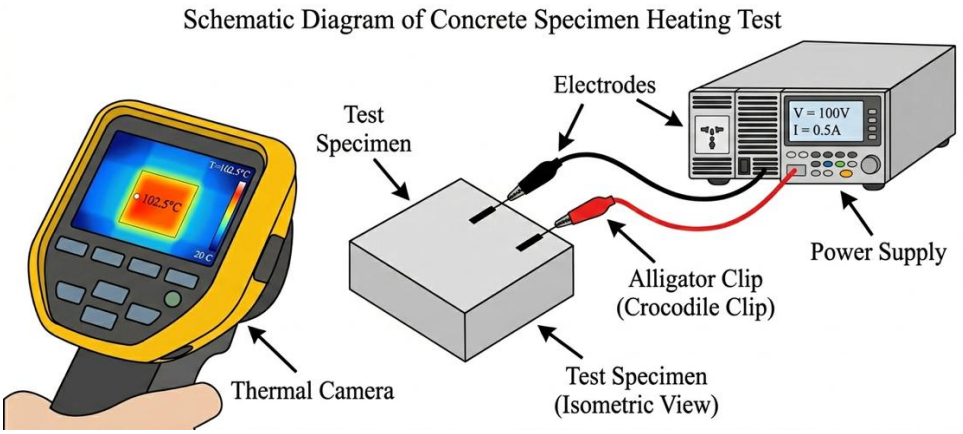

Figure 3. Self-heating measurement setup

Table 1. The specimen geometry, fiber properties, and experimental variables are summarized

Parameter	**Description / Value**
Specimen dimensions	150 × 150 × 50 mm³
Fiber bundle length	150 mm
Number of fiber bundles	4 (constant for all specimens)
Fibers per bundle	72k filaments

Parameter	Description / Value
Single fiber diameter	~7 μm
Fiber configurations	Straight, Twisted (Low–Medium–High), Braided (Low–Medium–High)
Cement : Aggregate : Water ratio	1 : 3 : 0.5
Electrical loading	AC, 30 V and 45 V
Temperature measurement	Infrared thermal camera

Electrical power consumption during the self-heating tests is determined from the measured voltage and current values. The instantaneous electrical power (P) dissipated within the specimens is calculated using the relationship:

$$P = V \times I \quad (1)$$

where V represents the applied AC voltage and I denotes the corresponding electrical current measured during testing. Voltage and current signals are recorded continuously, and power values are computed as a function of time. This approach allows direct evaluation of the electrical energy input associated with Joule heating under different fiber configurations and placement densities

3. Results and discussion

Hereafter, the terms low, medium, and high refer to the placement density of the fiber bundles unless otherwise stated. In the graphs, S, T, and B denote the fiber configurations, corresponding to straight, twisted, and braided carbon fiber bundles, respectively. The symbols L, M, and H indicate the placement density of the fiber bundles, defined as low, medium, and high. The applied electrical potentials are 30 V and 45 V**,** while the numerical values shown on the graphs represent the test duration in minutes.

3.1. Concrete Specimens with Four Continuous Carbon Fiber Bundles under 30 V

The self-heating behavior of concrete specimens containing four continuous carbon fiber bundles under an applied voltage of 30 V was evaluated by considering the effect of fiber configuration. Figure 4 presents the surface temperature evolution of the specimens for different configurations.

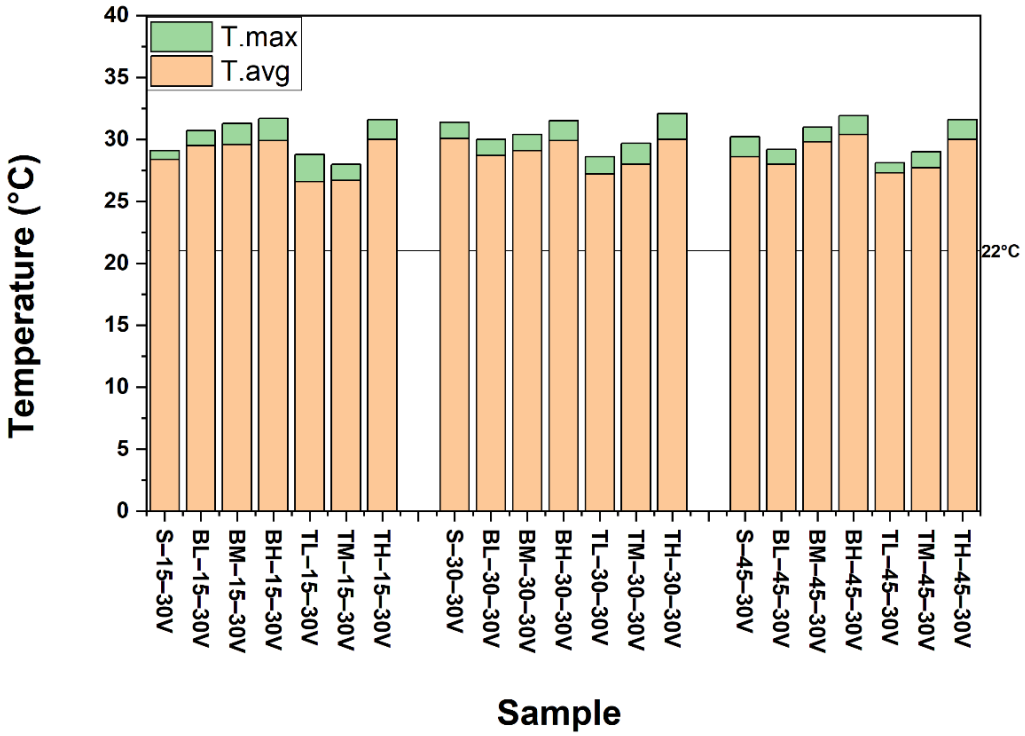

Figure 4. Surface temperature evolution of concrete specimens containing four continuous carbon fiber bundles under an applied voltage of 30 V, showing the effect of fiber configuration (straight, twisted, braided)

Among all cases, the braided–high configuration exhibited the highest thermal performance. At the end of the 45 min heating period, the surface temperature reached approximately 30.4 °C, which was higher than that of all other specimens (Figure 4). The twisted–high configuration showed a similar trend and reached a maximum temperature of about 30.0 °C, ranking second in terms of heating efficiency.

The braided–medium configuration demonstrated relatively good performance, with a final temperature of approximately 29.8 °C. In contrast, the braided–low and twisted–low specimens remained within the 27–28 °C range, indicating limited heat generation. The straight–low specimen reached a peak temperature of around 30.1 °C at 30 min; however, this value decreased to 28.6 °C by the end of the test, suggesting an unstable electrical network. Overall, these results indicate that braided fibers promote a more continuous electrical contact network, leading to enhanced Joule heating.

The electrical power consumption results under 30 V are shown in Figure 5. The observed trends are generally consistent with the temperature measurements. At 45 min, the braided–high configuration exhibited the highest power consumption, approximately 4.8 W, followed by the twisted–high configuration at about 4.5 W.

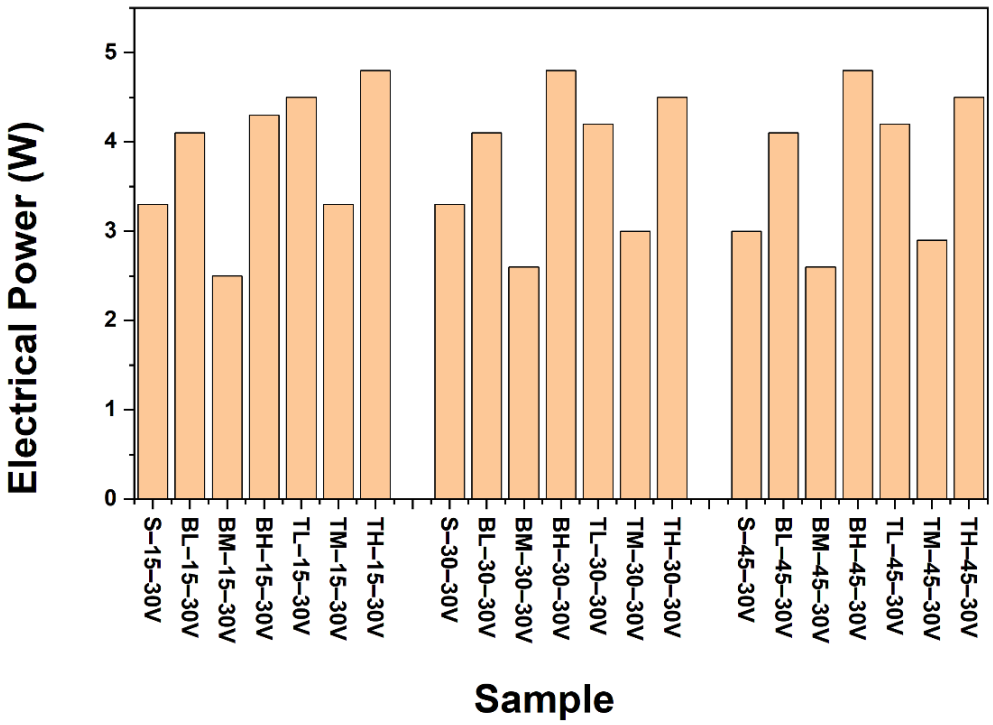

Figure 5. Electrical power consumption of concrete specimens reinforced with four continuous carbon fiber bundles under 30 V, as a function of fiber configuration (straight, twisted, braided)

Although the braided–medium specimen achieved relatively high temperatures, its power consumption remained low at around 2.6 W, indicating that temperature rise is not solely governed by electrical power input. The twisted–low specimen showed relatively high power consumption (~4.2–4.5 W) despite its limited temperature increase, suggesting inefficient conversion of electrical energy into uniform heating. The straight–low, braided–low, and twisted–medium configurations exhibited lower power consumption values. Based on these results, braided and twisted fibers with high placement density clearly provided the most efficient electrical and thermal performance under 30 V.

3.2. Concrete Specimens with Four Continuous Carbon Fiber Bundles under 45 V

Figure 6 illustrates the temperature evolution of the specimens subjected to an applied voltage of 45 V. Under this higher voltage level, the braided–medium and braided–high configurations exhibited the highest surface temperatures. At 45 min, the braided–medium specimen reached approximately 29.1 °C, while the braided–high specimen reached 29.2 °C, showing nearly identical performance.

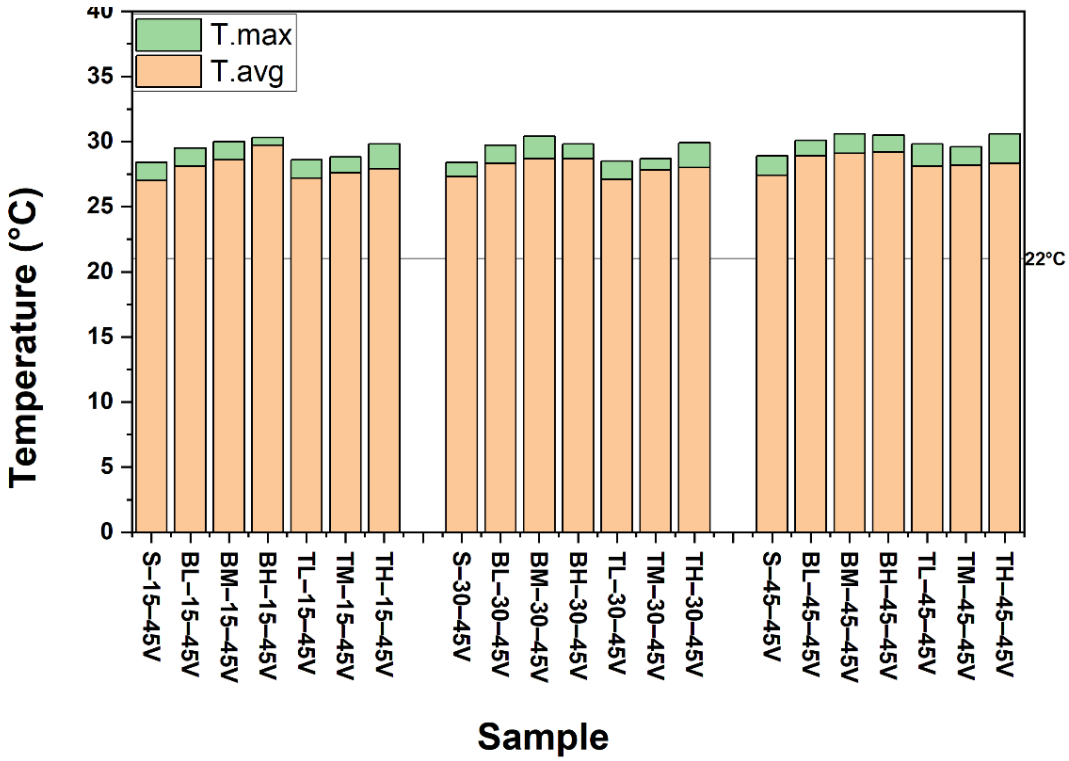

Figure 6. Surface temperature evolution of concrete specimens containing four continuous carbon fiber bundles subjected to an applied voltage of **45 V**, highlighting the influence of fiber configuration (straight, twisted, braided)

The braided–low configuration followed closely with a temperature of 28.9 °C. In comparison, the twisted–low and twisted–high specimens remained in the 28.1–28.3 °C range. The straight–low specimen exhibited the lowest temperature, reaching only 27.4 °C, while the twisted–medium configuration achieved a maximum temperature of 28.2 °C. These results confirm that braided fiber architectures are more effective in forming conductive networks that enhance Joule heating under higher voltage levels.

Electrical power consumption results at 45 V are presented in Figure 7. In contrast to the temperature trends, the highest power consumption was recorded for the twisted–low specimen, reaching approximately 4.3 W at 45 min (Figure 7). The braided–low configuration followed with a value of about 4.0 W. The braided–high and twisted–high specimens showed moderate power consumption levels of approximately 3.6 W.

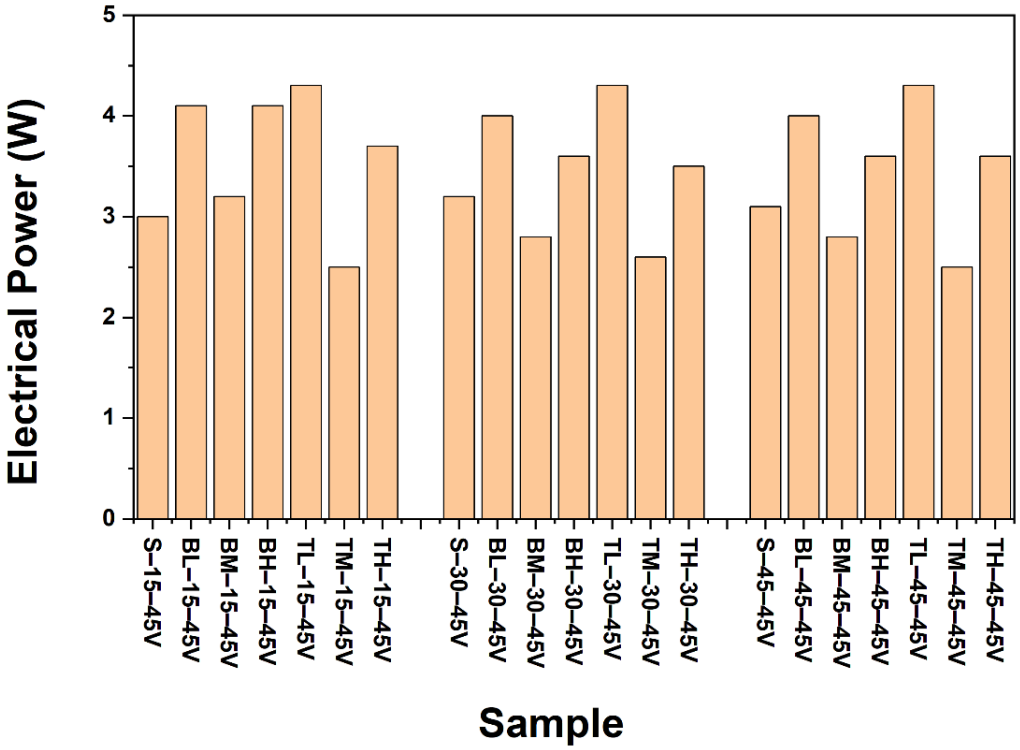

Figure 7. Electrical power consumption of concrete specimens reinforced with four continuous carbon fiber bundles under 45 V, for different fiber configurations (straight, twisted, braided)

Despite exhibiting one of the highest temperature increases, the braided–medium configuration consumed only ~2.8 W, while the twisted–medium specimen showed similarly low power consumption (~2.5 W). This discrepancy indicates that higher electrical power consumption does not necessarily result in higher surface temperatures and highlights the importance of conductive network uniformity and contact efficiency.

Considering both voltage levels, the results demonstrate that braided–high and twisted–high configurations consistently provide superior performance in terms of temperature increase and electrical behavior. The high placement density enhances fiber–fiber contact, improves electrical continuity, and promotes more effective Joule heating [26]. In contrast, low and medium density configurations tend to form less continuous conductive networks, resulting in reduced heating efficiency and lower temperature stability.

Although the braided–medium configuration achieved relatively high temperatures, its lower power consumption confirms that thermal output and electrical input are not always directly proportional. Overall, increasing the applied voltage improved the self-heating response [27], while braided fiber configurations with high density emerged as the most effective solution for achieving efficient and stable self-heating performance in cementitious composites.

4. Conclusion

This study examined the self-heating performance of concrete specimens incorporating four continuous carbon fiber bundles, focusing on the influence of fiber configuration and placement density under AC voltages of 30 V and 45 V. The results confirmed that continuous fiber architectures enable the formation of more effective and stable conductive networks compared to conventional dispersed systems.

Among all configurations, braided–high and twisted–high arrangements generally achieved higher temperature increases and more stable electrical behavior due to enhanced fiber–fiber contact and improved electrical continuity. In contrast, low and medium density configurations exhibited weaker conductive networks, leading to reduced heating efficiency. Although some medium-density braided specimens reached relatively high temperatures, their lower power consumption indicated that thermal output is strongly governed by network uniformity rather than electrical input alone.

Overall, the study demonstrates that fiber architecture selection is critical for achieving efficient self-heating performance in cementitious composites. Densely arranged continuous braided carbon fibers emerge as a promising solution for applications such as de-icing systems, heated pavements, and energy-efficient concrete-based heating elements.

Acknowledgements

The authors would like to express their sincere thanks to Omnea Abdulhamid Ali Elatrash for her valuable assistance during the experimental studies.

Funding

This study was supported by The Scientific and Technological Research Council of Turkey (TÜBİTAK) under the project number 224M051.

References

[1] Z. Li, X. Zhou, H. Ma, D. Hou, Advanced Concrete Technology, John Wiley & Sons, 2022.
[2] V.C. Li, High-Performance and Multifunctional Cement-Based Composite Material, Engineering 5 (2019) 250–260. https://doi.org/10.1016/j.eng.2018.11.031.
[3] H. Qin, S. Ding, A. Ashour, Q. Zheng, B. Han, Revolutionizing infrastructure: The evolving landscape of electricity-based multifunctional concrete from concept to practice, Progress in Materials Science 145 (2024) 101310. https://doi.org/10.1016/j.pmatsci.2024.101310.
[4] M.J. Abden, V.W.Y. Tam, J.D. Afroze, K.N. Le, Energy efficient sustainable concrete for multifunctional applications, Construction and Building Materials 418 (2024) 135213. https://doi.org/10.1016/j.conbuildmat.2024.135213.
[5] D.D.L. Chung, A review to elucidate the multi-faceted science of the electrical-resistance-based strain/temperature/damage self-sensing in continuous carbon fiber polymer-matrix structural composites, J Mater Sci 58 (2023) 483–526. https://doi.org/10.1007/s10853-022-08106-7.
[6] H. Zhang, G. Ju, L. Zhou, Q. Lu, X. Li, C. Su, X. Zheng, C. Su, B. Chen, L. Zhang, Mechanical-robust and polymer-based superhydrophobic coating toward self-cleaning and anti-corrosion, Journal of Cleaner Production 469 (2024) 143161. https://doi.org/10.1016/j.jclepro.2024.143161.
[7] S. Xue, S. Yang, X. Li, Q. Li, B. Hu, A comprehensive review on self-cleaning glass surfaces: durability, mechanisms, and functional applications, RSC Advances 14 (2024) 34390–34414. https://doi.org/10.1039/D4RA06680D.
[8] S. Sowmya, R.M.R. Pannem, Integrating bacteria and fibres for self-healing concrete: a comprehensive review of synergistic effects, Results in Engineering 28 (2025) 107071. https://doi.org/10.1016/j.rineng.2025.107071.
[9] L. Zhang, M. Zheng, D. Zhao, Y. Feng, A review of novel self-healing concrete technologies, Journal of Building Engineering 89 (2024) 109331. https://doi.org/10.1016/j.jobe.2024.109331.
[10] M. Siahkouhi, M. Rashidi, F. Mashiri, F. Aslani, M.S. Ayubirad, Application of self-sensing concrete sensors for bridge monitoring − A review of recent developments, challenges, and future prospects, Measurement 245 (2025) 116543. https://doi.org/10.1016/j.measurement.2024.116543.
[11] M. Civera, A. Naseem, B. Chiaia, Recent advances in embedded technologies and self-sensing concrete for structural health monitoring, Structural Concrete 26 (2025) 5300–5334. https://doi.org/10.1002/suco.202400714.
[12] S. Barbhuiya, B.B. Das, P. Norman, T. Qureshi, A comprehensive review of radiation shielding concrete: Properties, design, evaluation, and applications, Structural Concrete 26 (2025) 1809–1855. https://doi.org/10.1002/suco.202400519.
[13] B. Kanagaraj, N. Anand, S. Raj, E. Lubloy, Advancements and environmental considerations in portland cement-based radiation shielding concrete: Materials, properties, and applications in nuclear power plants– review, Cleaner Engineering and Technology 19 (2024) 100733. https://doi.org/10.1016/j.clet.2024.100733.
[14] S. Dong, X. Ouyang, F. Yu, B. Han, Self-heating curing and its influence on self-sensing properties of ultra-high performance concrete with hybrid stainless steel wires and steel fibers, Sensors and Actuators A: Physical 379 (2024) 115913. https://doi.org/10.1016/j.sna.2024.115913.

[15] W. Tian, X. Liu, Y. Liu, X. Wang, F. Zou, W. Cao, G. Guo, W. Wang, New insights into thermal-mechanical improvement of self-heating conductive high-performance cementitious composite, Construction and Building Materials 489 (2025) 142358. https://doi.org/10.1016/j.conbuildmat.2025.142358.
[16] L. do N. Farias, C.M. Ariani Fontes, J.H. Aquino Rocha, A.M. Dias, R.D. Toledo Filho, P.R. Lopes Lima, Bulk electrical resistivity of Concrete: Influence of sample size, moisture content, cracking, and composition, Journal of Building Engineering 107 (2025) 112744. https://doi.org/10.1016/j.jobe.2025.112744.
[17] W. Xu, K. Shu, D. Fan, R. Yu, Self-sensing enhancement in smart ultra-high performance concrete composites via multi-scale carbon black: Insights from micro to macro characteristics, Composites Part B: Engineering 304 (2025) 112645. https://doi.org/10.1016/j.compositesb.2025.112645.
[18] M. Shanbedi, A. Dashtbozorg, B. Safarianbana, Z. Heidari, A. Ebrahimi, Impact of raw and functionalized graphene on the mechanical and electrical performance of concrete, Innov. Infrastruct. Solut. 10 (2025) 547. https://doi.org/10.1007/s41062-025-02366-3.
[19] S. Onthong, W. Hanpongpun, S. Sinthupinyo, E.A. O'Rear, T. Pongprayoon, Bifunctional Multiwall Carbon Nanotubes and Their Effect on Hydration, Conductivity, and Mechanical Properties of Cement Composites, Int J Concr Struct Mater 19 (2025) 69. https://doi.org/10.1186/s40069-025-00812-1.
[20] G. Karalis, J. Zhao, M. May, M. Liebscher, I. Wollny, W. Dong, T. Köberle, L. Tzounis, M. Kaliske, V. Mechtcherine, Efficient Joule heaters based on mineral-impregnated carbon-fiber reinforcing grids: An experimental and numerical study on a multifunctional concrete structure as an electrothermal device, Carbon 222 (2024) 118898. https://doi.org/10.1016/j.carbon.2024.118898.
[21] S. Liu, J. Yang, Y. Yu, D. Liang, Y. Li, X. Si, S. Song, M. Meng, J. Zhang, Y. Zhang, Multifunctional flexible carbon fiber felt@nickel composite films with core–shell heterostructure: Exceptional Joule heating capability, thermal management, and electromagnetic interference shielding, Chemical Engineering Journal 494 (2024) 153221. https://doi.org/10.1016/j.cej.2024.153221.
[22] Z. Tan, F. Mahmood, M. Tian, Y. Li, Q. Zhang, Z. Ma, M. Wang, W. Liu, S. Zhang, H. Yang, B. Li, Review of Flash Joule Heating for the Synthesis of Graphene and Other Functional Carbon Materials, Carbon Energy n/a (n.d.) e70119. https://doi.org/10.1002/cey2.70119.
[23] X. Su, L. Ge, S. Huang, X. Wang, H. Xie, Y. Liu, L. Yi, L. Liu, J. Meng, H. Meng, Sustainable graphene from biomass via flash Joule heating: An innovative approach for cement mechanical performance, Biomass and Bioenergy 208 (2026) 108876. https://doi.org/10.1016/j.biombioe.2025.108876.
[24] J. Wang, J. An, Y. Li, Y. Xiang, Q. Xiao, Z. Tang, G. Long, Influencing factors of the temperature rise of direct electric curing concrete and its effect on concrete properties, Construction and Building Materials 438 (2024) 137110. https://doi.org/10.1016/j.conbuildmat.2024.137110.
[25] X. Liu, J. Wang, Z. Zhou, L. Zhang, Q. Fu, X. Liu, J. Wang, Z. Zhou, L. Zhang, Q. Fu, Gradient Joule Heating Curing Performance of Steel-Fiber-Reinforced High-Performance Concrete in Severe Cold Environments: A Preliminary Attempt for Deep-Cold Concrete Construction, Materials 18 (2025). https://doi.org/10.3390/ma18122909.
[26] L. Wang, S. Hou, W. Zhang, D. Zhang, J. Zhang, An innovative electromagnetic curing strategy for steel fiber-reinforced concrete: Thermal behavior, strength development, and microstructural evolution, Construction and Building Materials 494 (2025) 143395. https://doi.org/10.1016/j.conbuildmat.2025.143395.
[27] W. Dong, J. Zhao, B. Yang, M. Liebscher, V. Mechtcherine, Early strength enhancement of cementitious mineral-impregnated carbon fibre (MCF) reinforcements via electric Joule heating, Construction and Building Materials 489 (2025) 142231. https://doi.org/10.1016/j.conbuildmat.2025.142231.